Oxidative Stress Induces E-Selectin Expression through Repression of Endothelial Transcription Factor ERG

Jinjin Zhang,* Shuo Zhang,* Shanhu Xu,* Zhiying Zhu,* Jiang Li,* Zengjin Wang,† Youichiro Wada,‡ Alex Gatt,§,¶ and Ju Liu*,†

Oxidative stress induces a prothrombotic state through enhancement of adhesion properties of the endothelium. E-selectin, an endothelial cell adhesion molecule, becomes a therapeutic target for venous thrombosis, whereas the regulatory mechanisms of its expression have not been fully understood. In the present study, we report that H_2O_2 treatment increases expression of E-selectin but decreases expression of the endothelial transcription factor *ETS-related gene* (*ERG*) in HUVECs in a dose- and time-dependent manner. In BALB/c mice treated with hypochlorous acid, E-selectin expression is increased and ERG expression is decreased in endothelial cells of the brain and lung. RNA interference of *ERG* upregulates E-selectin expression, whereas transfection of ERG-expressing plasmid downregulates E-selectin expression in HUVECs. Knockdown or overexpression of ERG comprises H_2O_2-induced E-selectin expression in HUVECs. Deletion of the *Erg* gene in mice results in embryonic lethality at embryonic days 10.5–12.5, and E-selectin expression is increased in the $Erg^{-/-}$ embryos. No chromatin loop was found on the *E-selectin* gene or its promoter region by capture high-throughput chromosome conformation capture. Chromatin immunoprecipitation and luciferase reporter assay determined that the −127 ERG binding motif mediates ERG-repressed *E-selectin* promoter activity. In addition, ERG decreases H_2O_2-induced monocyte adhesion. Together, ERG represses the *E-selectin* gene transcription and inhibits oxidative stress–induced endothelial cell adhesion. *The Journal of Immunology*, 2023, 211: 1835–1843.

E-selectin, also known as CD62E, is a glycoprotein specifically expressed on endothelial cells (1). Upon activation of proinflammatory cytokines, expression of E-selectin is rapidly upregulated (1, 2). The lectin-EGF elements of E-selectin recognize glycoproteins or glycolipids on leukocytes' surface (3), which include P-selectin glycoprotein ligand-1, E-selectin ligand-1, and CD44 (4–6). E-selectin promotes leukocyte tethering, rolling along the endothelium and facilitating leukocyte transmigration (7, 8). E-selectin mediates leukocyte adhesion to endothelial cells and also augments thrombotic clot formation as the fibrin content (9). Inhibition of E-selectin reduces venous thrombosis and prevents fibrin formation (10). Circulating E-selectin (soluble E-selectin) is formed by enzymatic cleavage of transmembranous E-selectin on activated endothelial cells (11). The concentration of soluble E-selectin is directly correlated with cell surface expression (12) and increases upon endothelial cell injury (13, 14).

Oxidative stress is induced with uncontrolled production of reactive oxygen species (ROS) (15). Excessive ROS causes an increase of subendothelial low-density lipoprotein cholesterol (LDL), which is oxidized to form oxidized LDL (ox-LDL) (16). ox-LDL increases expression of adhesion molecules such as ICAM-1 and VCAM-1, resulting in leukocyte adhesion and migration through the endothelium (17). Hyperglycemia also increases the production of ROS and increases leukocyte adhesion by upregulation of adhesion molecules (18, 19). In hypertension, angiotensin II induces extra production of ROS in endothelial cells (20) and upregulates E-selectin expression in endothelial cells (21). In addition, oxidative stress induces thrombus formation, which requires leukocyte adhesion and enhances adhesion molecule expression (22, 23). A mouse model of venous thrombosis showed more neutrophils in the vein wall (24). Attachment of neutrophils to endothelial cells is regulated by adhesion molecules, including E-selectin (25). However, modulation of E-selectin expression in oxidative stress–induced thrombosis formation has not been explored.

The *ETS-related gene* (*ERG*) belongs to the E-26 transformation-specific family of transcription factors by recognizing the conserved binding motif GGAA/T (26). ERG is specifically expressed in the endothelial cells and maintains the vascular barrier function through transcriptional regulation of the expression of VE-cadherin (27), endoglin (28), and claudin-5 (29). Deletion of the *ERG* gene in mice led to embryonic lethality at embryonic days 10.5–12.5 with vascular defects and hemorrhage (30). In addition, ERG is required for expression of coagulation-related factors von Willebrand factor (31) and thrombomodulin (32). ERG also maintains vascular homeostasis through inhibition of adhesion molecule ICAM-1 (33).

*Medical Research Center, Shandong Provincial Qianfoshan Hospital, Shandong University, Jinan, China; †Institute of Microvascular Medicine, Medical Research Center, The First Affiliated Hospital of Shandong First Medical University & Shandong Provincial Qianfoshan Hospital, Jinan, China; ‡Isotope Science Center, The University of Tokyo, Tokyo, Japan; §Department of Pathology, Faculty of Medicine and Surgery, University of Malta, Tal-Qroqq, Msida, Malta; and ¶Hematology Laboratory, Department of Pathology, Mater Dei Hospital, Msida, Malta

ORCIDs: 0000-0001-6255-8972 (Z.Z.); 0000-0003-4543-5991 (Y.W.); 0000-0002-4314-048X (A.G.); 0000-0001-9932-2613 (J.L.).

Received for publication January 18, 2023. Accepted for publication October 12, 2023.

This work was supported by the National Natural Science Foundation of China (82171318, 82241030), the Academic Promotion Program of Shandong First Medical University (2019QL014), and the Shandong Taishan Scholarship (to J.L.).

J.Z., S.Z., and J.L. performed experiments and analyses. J.Z., S.Z., S.X., Z.Z., J.L., Z.W., and J.L. collected and interpreted the data. J.Z., Y.W., A.G., and J.L. wrote and edited the manuscript. All authors approved the final version of the manuscript.

Address correspondence and reprint requests to Prof. Ju Liu, Medical Research Center, Shandong Provincial Qianfoshan Hospital, Shandong University, 16766 Jingshi Road, Jinan, Shandong, China 250014. E-mail address: ju.liu@sdu.edu.cn

The online version of this article contains supplemental material.

Abbreviations used in this article: CHi-C, capture high-throughput chromosome conformation capture; ChIP, chromatin immunoprecipitation; CM, culture medium; ERG, ETS-related gene; HOCl, hypochlorous acid; LDL, low-density lipoprotein cholesterol; ox-LDL, oxidized low-density lipoprotein cholesterol; qRT-PCR, quantitative RT-PCR; ROS, reactive oxygen species; SELE, E-selectin; SELL, L-selectin.

https://doi.org/10.4049/jimmunol.2300043

In this study, we report that H_2O_2 stimulation increases E-selectin expression and decreases ERG expression in a dose- and time-dependent manner in cultured endothelial cells. In mice, hypochlorous acid (HOCl) treatment increases E-selectin expression while decreasing ERG expression in endothelial cells of the brain and lung. ERG negatively regulates E-selectin expression in cultured endothelial cells and in mouse embryos, whereas it mediates H_2O_2-induced E-selectin expression. ERG regulates the *E-selectin* promoter activity through the −127 ERG binding motif. In addition, ERG decreases H_2O_2-induced monocyte attachment on endothelial cells. Our findings demonstrate ERG represses the *E-selectin* gene transcription on endothelial cells, and it represents what is, to our knowledge, a novel mediator for oxidative stress–induced adhesion.

Materials and Methods

Animal models

A total of 20 female BALB/c mice at 6 wk of age were obtained from Vital River (Beijing, China) and randomly divided into the PBS control group and the HOCl treatment group. The HOCl treatment was performed as previously described (34). Briefly, HOCl was freshly prepared by adding NaClO solution (active chlorine 6%) to KH_2PO_4 solution (100 mM; pH 6.2). A dosage of 200 μl HOCl solution was injected intradermally into the shaved back of the mouse by a 27-gauge needle once every day for 8 wk. The control group of mice was injected with 200 μl sterilized PBS. The chemical reagents were obtained from Solarbio (Beijing, China). The $Erg^{+/-}$ mice were generated by Gem Pharmatech (Nanjing, China) through CRISPR/Cas9 technology. Two guide RNAs, 5′-AGCACCTTTACCTGCGCCTT-3′ and 5′-GAATCTCCTTGGTAGTAGGT-3′, were constructed to delete the 683-bp fragment spanning exons 4–10 of the *Erg* gene and were introduced with Cas9 nuclease into the C57BL/6NJ-derived fertilized eggs, followed by transfer to pseudopregnant females. Mouse genotyping was confirmed by PCR, and primer sequences are listed in Supplemental Table I. All experimental studies were performed in accordance with guidelines prescribed by the animal care committee of Shandong University.

Cell culture and transfection

HUVECs were purchased from ScienCell (Carlsbad, CA) and cultured in basal endothelial cell medium supplemented with the EGM-2-MV bullet kit (ScienCell). THP-1 monocytes were purchased from the American Type Culture Collection and cultured in RPMI 1640 (Life Technologies, Waltham, MA) supplemented with 10% FBS (Life Technologies). The siRNAs were synthesized by GenePharma (Shanghai, China): NC siRNA, 5′-UUCUCCGAACGUGUCACGUTT-3′; ERG siRNA, 5′-GGACAGACUUCCAAGAUGATT-3′. pcDNA3-ERG plasmid was obtained from OriGene Technologies (catalog no. RC208093; Rockville, MD). HUVECs of passages 4–8 were grown to 70% confluence and transfected with 50 nmol siRNAs or 2 μg pERG plasmid with Lipofectamine 2000 reagent according to the manufacturer's instructions (Thermo Fisher Scientific, Waltham, MA).

Real-time PCR

Total RNA was isolated from cells and tissues using TRIzol reagent (Invitrogen, Carlsbad, CA). The cDNA was synthesized with the Hi SuperScript Reverse Transcriptase Kit (Vazyme, Nanjing, China). Quantitative RT-PCR (qRT-PCR) was carried out using the Bio-Rad CFX96 Real-Time System (Bio-Rad Laboratories, Hercules, CA) with SYBR Green PCR Master Mix (Vazyme). The fold change was calculated by the $2^{-\Delta\Delta Ct}$ method. The primer sequences are shown in Supplemental Table I.

Western blot analysis

Cells and mouse tissues were collected in ice-cold radioimmunoprecipitation assay/0.1% SDS lysis buffer supplemented with 1% PMSF (Wuhan, China). An equal amount of protein sample was separated by 10% SDS-PAGE (Bio-Rad

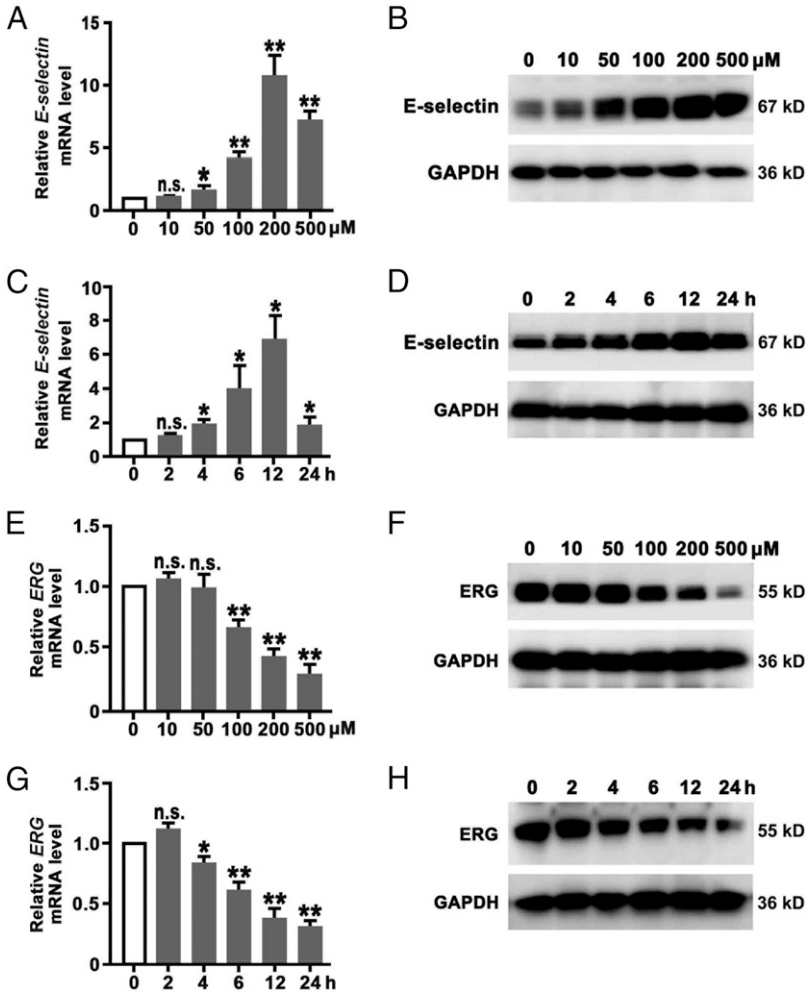

FIGURE 1. H_2O_2 increases E-selectin expression and decreases ERG expression in HUVECs in a dose- and time-dependent manner. HUVECs were treated with 0, 10, 50, 100, 200, or 500 μM H_2O_2 for 12 h. Expression of mRNA of the *E-selectin* (**A**) and *ERG* (**E**) genes was determined by qRT-PCR. The protein levels of E-selectin (**B**) and ERG (**F**) were determined by Western blotting ($n = 5$). HUVECs were treated with 200 μM H_2O_2 for 0, 2, 4, 6, 12, or 24 h. E-selectin expression was assessed by qRT-PCR (**C**) and Western blotting (**D**). Expression of mRNA of the *E-selectin* (C) and *ERG* (**G**) genes was determined by qRT-PCR. The protein levels of E-selectin (D) and ERG (**H**) were determined by Western blot analysis ($n = 5$). GAPDH was used as a loading control. $^*p < 0.05$, $^{**}p < 0.01$.

Laboratories) and then transferred onto a PVDF membrane (EMD Millipore, Burlington, MA). The membrane was blocked in TBST solution containing 5% nonfat milk for 1 h and then incubated with the primary Ab overnight at 4°C. After washing, the membrane was incubated with the HRP-conjugated secondary Ab for 1 h. Protein bands were visualized by the GE Amersham Imager 600 (GE Healthcare Bio-Sciences, Marlborough, MA). Densitometry of immunoblots was quantified by ImageJ software (NIH, Bethesda, MD). The primary Abs were as follows: E-selectin (10494-1-AP, 1:500; PTG, Rosemont, PA), ERG (92513, 1:1000; Abcam, Boston, MA), and GAPDH (10494-1-AP, 1:8000; PTG). The secondary Abs were goat anti-rabbit IgG (SA00001-2, PTG) and goat anti-mouse IgG (SA00001-1, PTG).

Immunofluorescence

Mouse brain and lung tissues were frozen in O.C.T. compound (Sakura Finetek, Torrance, CA), cut at 7 μm, and placed on slides. After fixation with cold methyl alcohol, the slides were incubated with primary Abs overnight at 4°C and then stained with fluorescent secondary Abs for 1 h at room temperature. Then, the slides were incubated with DAPI (Solarbio Technology, New York, NY) for nuclear staining for 5 min. The staining was photographed using a Leica upright microscope (Leica, Wetzlar, Germany). The primary Abs were as follows: CD31 (1:50; BD Biosciences, Franklin Lakes, NJ), ERG (1:200; Abcam), E-selectin (1:200; PTG). The secondary Abs were goat anti-rabbit Alexa Fluor 488 (1:200; Abcam) and goat anti-rat Alexa Fluor 546 (1:50; Invitrogen).

Capture high-throughput chromosome conformation capture

HUVECs were fixed with 1% formaldehyde for 10 min, and then 0.2 M glycine was used to quench the cross-linking for 5 min. Next, capture high-throughput chromosome conformation capture (CHi-C) was performed according to previously described protocols (35). To generate the CHi-C library, biotin-labeled 120-bp RNA baits were targeted to the promoter of the *SELE* (*E-selectin*) gene and its neighboring gene *SELL* (*L-selectin*) (chr1:169676615-169676734, chr1:169702595-169702714, chr1:169706244-169706363). The CHi-C library was sequenced on the Illumina NovaSeq 6000 platform, and the analysis of sequencing data was performed as previously described (36, 37).

Chromatin immunoprecipitation

HUVECs were cross-linked with 1% formaldehyde for 10 min. Chromatin immunoprecipitation (ChIP) was performed according to the manufacturer's instructions (9005s; Cell Signaling Technology, Danvers, MA). Immunoprecipitation was performed overnight at 4°C with anti-ERG Ab (133264; Abcam) or IgG (3900; Cell Signaling Technology). The purified DNA fragments were analyzed by semiquantitative PCR and qRT-PCR. The primer sequences are shown in Supplemental Table I.

THP-1–HUVEC adhesion assay

HUVECs were treated with H_2O_2 and/or transfected with ERG siRNA or pERG. THP-1 cells were incubated with 10 μM calcein-AM (Thermo Fisher) at 37°C for 15 min and then added to HUVEC culture medium (CM) at 1×10^6 cells/ml. After incubation for 30 min, the nonadherent THP-1 cells were removed by rinsing with PBS. The adherent THP-1 cells labeled by calcein-AM were captured by fluorescence microscopy (Leica).

ELISA

After transfection with siERG or pERG plasmids for 48 h, the CM of HUVECs was collected and centrifuged for 5 min at $180 \times g$. The supernatant was collected and measured by an E-selectin ELISA kit following the manufacturer's protocol (DSLE00; R&D Systems, Minneapolis, MN).

Luciferase activity

The fragment spanning the region −840 to +1 of the *E-selectin* promoter was synthesized by SangonBiotech (Shanghai, China) and subcloned into the pGL3-basic plasmid through the XhoI/HindIII digestion sites. The mutation

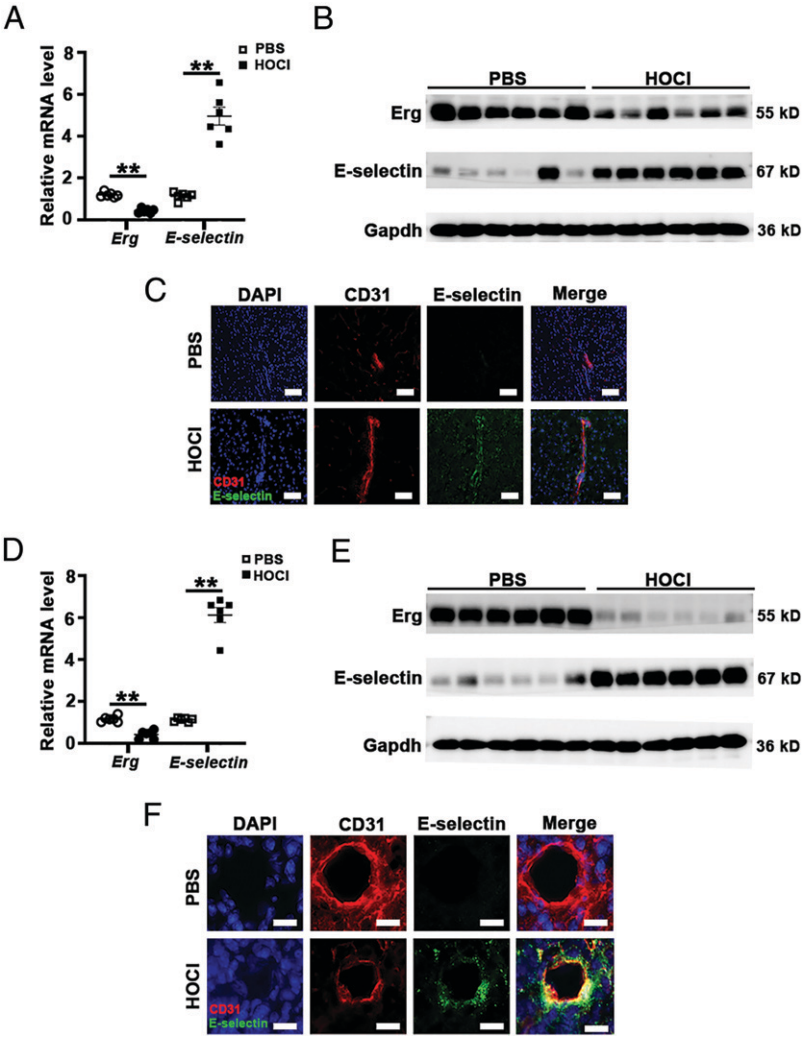

FIGURE 2. The expression of Erg and E-selectin in mice treated with HOCl. Mice were administered an injection with HOCl to induce oxidative stress. Expression of mRNA levels of the *Erg* and *E-selectin* genes in brains (**A**) or lungs (**D**) was detected by qRT-PCR ($n = 6$). $^{**}p < 0.01$. The protein levels of Erg and E-selectin in brains (**B**) or lungs (**E**) were detected by Western blot analysis ($n = 6$). GAPDH was used as a loading control. (**C** and **F**) Representative images of double-immunofluorescence staining of CD31 (red)/E-selectin (green) on brain (C) or lung (F) tissue. Scale bars, 50 μm.

of the −127 *ERG* binding site was generated (5′-TTCCCGGGAA-3′ to 5′-GTAACGTAGA-3′). The pGL3-*E-selectin* (*WT*) and pGL3-*E-selectin* with *ERG* mutation (*ERG mut*) plasmids were transfected into HUVECs with Lipofectamine 3000 (Thermo Fisher) following the manufacturer's protocol. The pCMV-TK was used as an internal control. Luciferase activity was measured using the Dual-Glo luciferase reporter assay system (Promega, Madison, WI), and the light intensity was measured by a Berthold luminometer (Wildbad, Germany). The relative luciferase activity was normalized to internal Renilla luciferase activity.

Statistical analysis

All statistical analyses were performed using GraphPad Prism software version 9.0c (GraphPad Software, La Jolla, CA). Data obtained were exhibited as the mean ± SEM. Comparison between two groups was determined by unpaired Student *t* test. A value of $p < 0.05$ was considered to indicate a statistically significant difference.

Results

H_2O_2 treatment increases E-selectin expression and decreases ERG expression in HUVECs in a dose- and time-dependent manner

HUVECs were treated with 0, 10, 50, 100, 200, or 500 μM H_2O_2 for 12 h to induce oxidative stress. All concentrations of H_2O_2-stimulated intracellular ROS production were measured by DCFH-DA (Supplemental Fig. 1A). Expression of E-selectin and ERG in H_2O_2-treated HUVECs was determined by qRT-PCR (Fig. 1A, 1E) and Western blot analysis (Fig. 1B, 1F). Expression of E-selectin was increased with a peak at 200 μM H_2O_2 treatment. Next, HUVECs were exposed to 200 μM H_2O_2, and mRNA and protein were collected at 0, 2, 4, 6, 12, and 24 h for examination for E-selectin expression. Fig. 1C and 1D show that mRNA and protein levels of E-selectin expression are increased with a maximal level at 12 h. In the same sets of HUVECs, qRT-PCR and Western blotting showed that expression of transcription factor ERG is decreased at 100, 200, and 500 μM H_2O_2 treatment for 12 h, and its expression is also decreased upon 200 μM H_2O_2 treatment at 4, 6, 12, and 24 h (Fig. 1G, 1H). The intensity of protein bands was quantified by normalization to GAPDH (Supplemental Fig. 2A–2D). Together, H_2O_2 treatment increases E-selectin expression and decreases ERG expression in a dose- and time-dependent manner in HUVECs.

Oxidative stress induction increases E-selectin expression while decreasing ERG expression in mice

In vivo oxidative stress was induced by injection of HOCl into mice and validated by malondialdehyde assay (Supplemental Fig. 1B). The expression of E-selectin and ERG mRNA and protein levels in mouse brain and lungs was assessed by qRT-PCR and Western blot analysis. In HOCl-treated mouse brain and lung tissues, mRNA and protein levels of E-selectin were significantly increased, whereas mRNA and protein levels of ERG were significantly decreased (Fig. 2A, 2B, 2D, and 2E). In addition, double-immunofluorescence staining of CD31/E-selectin was performed on mouse tissues. In endothelium positively stained for CD31, the intensity of E-selectin staining was significantly increased, whereas the staining of ERG was significantly decreased, in brain (Fig. 2C) and lung tissues (Fig. 2F) of HOCl-treatment mice.

ERG negatively regulates E-selectin expression in HUVECs

To determine the role of ERG in the regulation of E-selectin expression, ERG expression was knocked down by siRNA interference in HUVECs and validated by qRT-PCR and Western blot analysis (Fig. 3). In HUVECs with knockdown of ERG expression, mRNA and protein levels of E-selectin were significantly increased (Fig. 3A, 3B). To detect the soluble E-selectin, ELISA was performed with the CM, and no significant difference was found in the CM of HUVECs transfected with ERG siRNA and scrambled RNA (Fig. 3C). In addition, ERG-expressing plasmid (pERG) was transfected in HUVECs, and ERG overexpression was validated by qRT-PCR and Western blot analysis. In HUVECs with ERG overexpression, mRNA and protein levels of E-selectin were decreased (Fig. 3D, 3E), whereas the soluble E-selectin in CM remained unchanged (Fig. 3F). The intensity of protein bands was quantified by normalization to GAPDH (Supplemental Fig. 2E, 2F). In HUVECs transfected with ERG siRNA, H_2O_2 treatment did not induce an additional increase of E-selectin expression (Fig. 3G). In HUVECs transfected with pERG

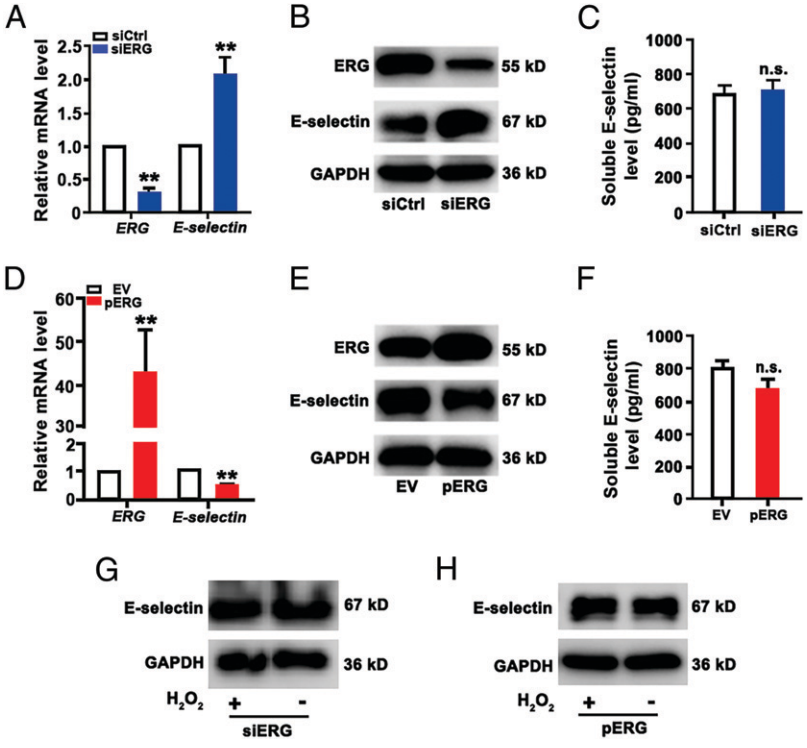

FIGURE 3. ERG represses E-selectin expression in HUVECs. HUVECs were transfected with ERG siRNAs (**A**–**C**) or ERG-expressing plasmids (**D**–**F**). (A and D) Expression of mRNA of the *ERG* and *E-selectin* genes was detected by qRT-PCR ($n = 5$). (B and E) The protein levels of ERG and E-selectin were examined by Western blotting ($n = 5$). (C and F) The concentrations of E-selectin in the CM were determined by ELISA. (**G** and **H**) HUVECs were transfected with ERG siRNA or pERG plasmids for 24 h and then treated with 200 μM H_2O_2 for 12 h. The protein levels of E-selectin were detected by Western blot analysis. GAPDH was used as a loading control. $^{**}p < 0.01$. EV, empty vector.

plasmid, H_2O_2 treatment failed to increase E-selectin expression (Fig. 3H). Thus, E-selectin expression in endothelial cells is negatively regulated by ERG, which mediates oxidative stress–induced E-selectin expression.

Deletion of the Erg gene in mice increases the expression of E-selectin

To validate the role of ERG in E-selectin expression in vivo, $Erg^{+/-}$ mice were generated by CRISPR/Cas9 technology. Homogeneous deletion of the *Erg* gene resulted in embryonic lethality (30). The $Erg^{+/-}$ mice were intercrossed to obtain the $Erg^{-/-}$ embryos, which were validated by PCR of the genomic DNA from the yolk sac (Fig. 4B). Fig. 4C shows representative images of E11.5 $Erg^{+/+}$ and $Erg^{-/-}$ embryos with or without yolk sacs. The mRNA and protein of the embryos were collected to examine E-selectin expression. In the $Erg^{-/-}$ embryos, transcription of the E-selectin gene and E-selectin protein level were significantly increased (Fig. 4D, 4E).

Chromatin interaction is absent on the E-selectin promoter

Previous studies have reported endothelium-specific genes are regulated by chromatin looping structures between enhancers and promoters (38–41). To explore chromatin regulation of the gene transcription, promoter CHi-C was performed for the *E-selectin* gene and its neighboring gene *SELL* using a biotinylated RNA bait library designed for human GRCh37/hg19 genomes (35). Three promoter-interacting regions were identified to interact with the *SELL* promoter (Fig. 5A), and these promoter-interacting regions are located on the adjacent genes *SELP* and *F5* (Fig. 5B). However, no chromatin interaction was captured on the *E-selectin* promoter on a genome-wide scale (Fig. 5A, 5B). Therefore, the *E-selectin* gene transcription is not governed by interactions of promoters with distal elements through chromatin loops.

ERG directly binds to the E-selectin promoter and represses the promoter activity in HUVECs

The conservation of the regulatory elements of the *E-selectin* gene promoter were predicted by the University of California Santa Cruz Genome tool (http://genome.ucsc.edu), and the consensus sequence −127 ERG binding element was identified (Supplemental Fig. 3). The 840 kb upstream of the transcription start site of the *E-selectin* gene was cloned, and the −127 ERG binding site was

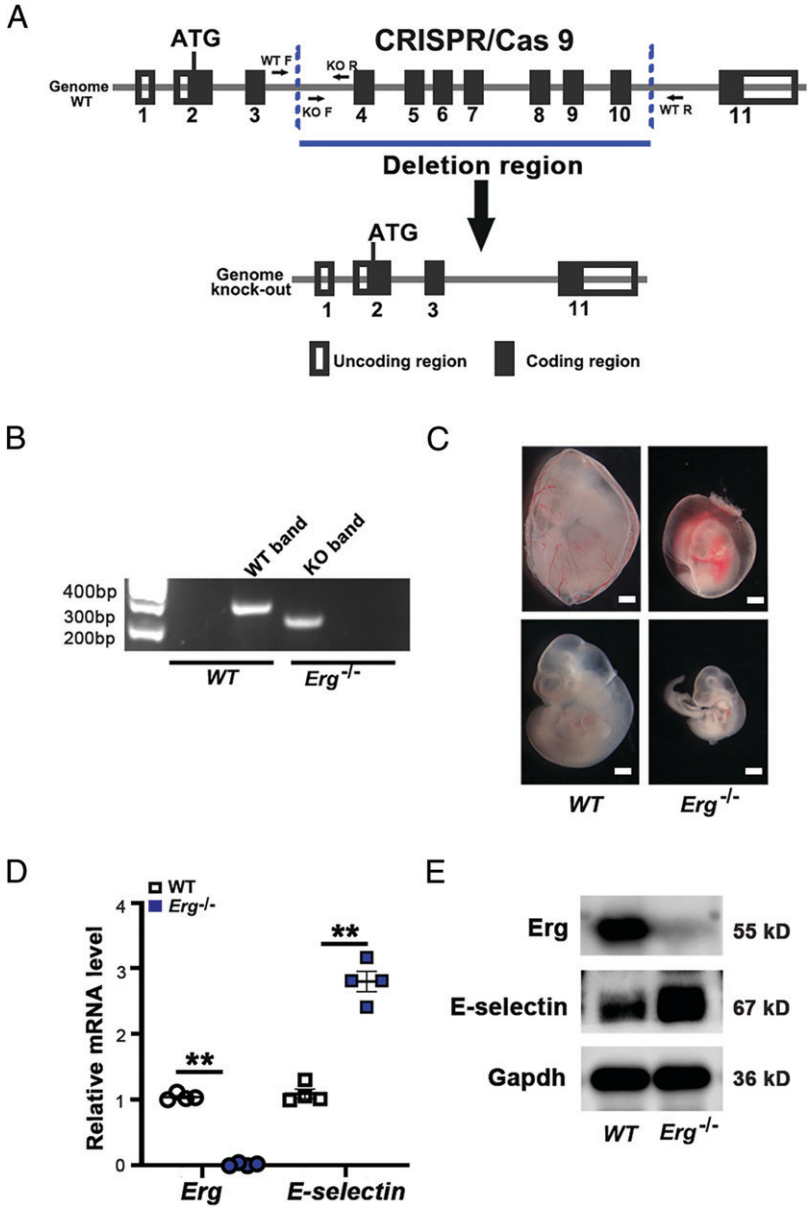

FIGURE 4. Deletion of the *Erg* gene in mice increases expression of E-selectin. (**A**) The schematic strategy to construct the $Erg^{-/-}$ mice. CRISPR/Cas9 sgRNA genome targeting the exons 4–10 region of the *Erg* gene. KO, knockout; WT, wild type. (**B**) Validation of gene targeting of the *Erg* gene by PCR. (**C**) Representative images of embryonic day 11.5 *WT* and $Erg^{-/-}$ embryos with or without yolk sacs. Scale bar, 500 μm. (**D**) Expression of mRNA of the *Erg* and *E-selectin* genes in the embryonic day 11.5 *WT* and $Erg^{-/-}$ embryos ($n = 4$). Data are shown as mean ± SEM. $^{**}p < 0.01$. (**E**) Immunoblots of Erg and E-selectin proteins from the embryonic day 11.5 *WT* and $Erg^{-/-}$ embryos.

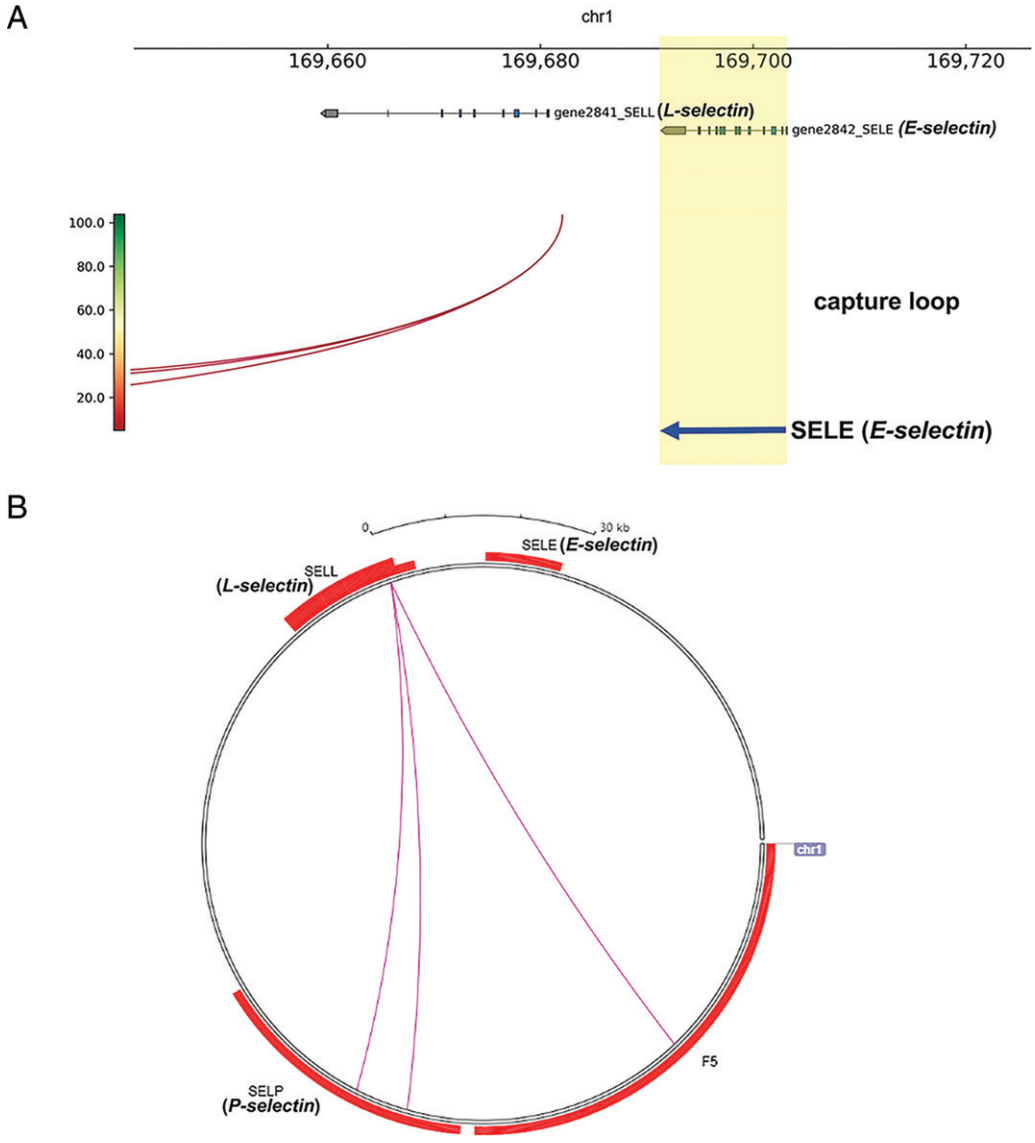

FIGURE 5. CHi-C analyses of the *E-selectin* (*SELE*) gene. (**A**) Chromatin interactions on 169660–169720 kb on chromosome 1. The *E-selectin* (*SELE*) and *L-selectin* (*SELL*) genes are shown as red arcs. The yellow highlight is the location of the *SELE* gene. The blue arrow is the direction of *SELE* transcription. (**B**) Circlet view of CHi-C interactions. Gene density is in red and the link of *cis*-regulated elements. The figure was generated using WashU Epigenome Browser, GRCh37/hg19.

mutated (Fig. 6A, left). Both fragments were cloned into the pGL3 construct and transfected into HUVECs with pERG or empty vector (Fig. 6A, right). Luciferase assays showed that overexpression of ERG significantly decreased the *E-selectin* promoter activity (Fig. 6A, right). In addition, mutation of the −127 ERG binding site significantly increased the *E-selectin* promoter activity and compromised ERG-induced inhibition of the promoter activity. ChIP was performed with ERG Ab on the −127 ERG binding motif on the *E-selectin* promoter region in HUVECs transfected with pERG or empty vector. As shown in Fig. 6B and 6C, ERG directly binds to the *E-selectin* promoter, and binding affinity is significantly increased with overexpression of ERG. These results indicated that ERG interacts with the −127 ERG binding motif and inhibits the *E-selectin* promoter activity.

ERG decreases THP-1 cell adhesion to HUVECs

In mice treated with HOCl, leukocyte adhesion to the vascular wall is increased, as shown by H&E staining (Supplemental Fig. 1C). In vitro, HUVECs were incubated with 200 μM H_2O_2 for 6 h, and THP-1 cells were added into the culture for 30 min. After washing, we found that the number of THP-1 cells adhered to HUVECs was significantly increased by H_2O_2 treatment (Fig. 7A). These results confirmed that oxidative stress increases monocyte adhesion to endothelial cells. Transfection with ERG siRNA in HUVECs resulted in a significant increase of THP-1 cell adhesion (Fig. 7B), whereas transfection with pERG in HUVECs significantly reduced THP-1 cell adhesion (Fig. 7C). In HUVECs transfected with ERG siRNA, H_2O_2 treatment failed to induce an additional increase in the number of adhered THP-1 cells (Fig. 7D). Thus, ERG negatively regulates monocyte adhesion to endothelial cells (Fig. 8).

Discussion

In this study, we found that oxidative stress increases E-selectin expression, whereas it decreases ERG expression in endothelial cells both in vitro and in vivo. ERG represses E-selectin expression in HUVECs, and the $Erg^{-/-}$ mouse embryos showed elevated E-selectin expression. In addition, ERG directly binds to the *E-selectin* promoter and inhibits the promoter activity. Knockdown of ERG expression in endothelial cells compromises oxidative stress–induced monocyte adhesion.

Oxidative stress with overproduction of ROS initiates endothelial dysfunction, leading to vascular diseases. ox-LDL, angiotensin II, and hyperglycemia increase adhesion molecule expression and subsequent leukocyte adhesion, which is likely mediated by extra production of ROS (17, 20, 21, 42–44). In addition, H_2O_2 treatment

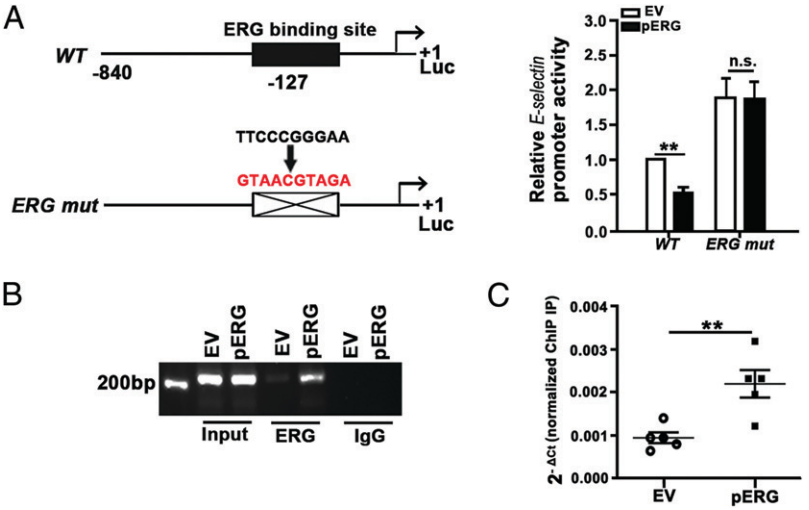

FIGURE 6. ERG suppresses the *E-selectin* promoter activity in HUVECs. (**A**) Schematic representation of the E-selectin promoter-driven luciferase reporter constructs (left). HUVECs were transfected with pGL3-E-selectin (*WT*) or pGL3-E-selectin (mutation of the −127 ERG motif) with EV or pERG plasmids, and the luciferase activity was measured (right) ($n = 5$). (**B** and **C**) ChIP assay for ERG binding to the *E-selectin* promoter in HUVECs transfected with EV and pERG plasmid. (B) Representative image of semiquantative PCR of the DNA fragments pulled down by ChIP assay with ERG Ab. (C) qRT-PCR analysis of the DNA fragments pulled down by ChIP assay with ERG Ab ($n = 5$). $^{**}p < 0.01$. EV, empty vector.

promotes polymorphonuclear neutrophil adhesion to HUVECs (45). In this study, we found that H_2O_2 treatment directly increased E-selectin expression and promoted monocyte adhesion to endothelial cells, supporting the role of E-selectin in oxidative stress–induced endothelial cell adhesion.

Oxidative stress promotes blood cell–endothelial cell interactions to facilitates vascular thrombus formation (46). The composition of vascular thrombi includes fibrin, RBCs, platelets, leukocytes, and neutrophil extracellular traps (47). Leukocyte infiltration in the vein wall is related to vascular thrombus weight (48). In a venous thrombosis mouse model established by ligation of the infrarenal inferior vena cava, E-selectin mRNA and protein levels were increased in mouse inferior vena cava tissues (48). In the same thrombotic mouse model, *E-selectin*$^{-/-}$ mice showed less neutrophil adhesion than the wild-type clotted animal (9, 48), suggesting that E-selectin facilitates clot formation during venous thrombosis. GMI-1271, a small glycomimetic antagonist for E-selectin (49), was found to be safe and effective for the treatment of calf vein deep vein thrombosis (49, 50). Our study also supports that E-selectin is a therapeutic target for thrombosis. Recent studies discovered that transcription of multiple genes was modulated by chromatin interaction (38–41). In our study, no loop was found on the *E-selectin* gene and promoter region by CHi-C. This excluded the role of chromatin interaction in regulation of the E-selectin gene transcription.

Previous studies reported that the E-selectin gene expression is upregulated by transcription factors, including NF-κB, activating transcription factor 2, and high-mobility group protein I (Y) (51–54). In addition, the −195 AP1 and −90 Ets-1 binding sites on the *E-selectin* promoter mediate K1-3 regulated *E-selectin* gene transcription (55). In this study, we performed phylogenetic analysis and identified a highly conserved ERG binding motif at the −127 site on the E-selectin promoter. Mutation of this motif increases the *E-selectin* promoter activity and abolishes ERG-induced decrease of the *E-selectin* promoter activity. A ChIP assay showed that ERG directly binds to the

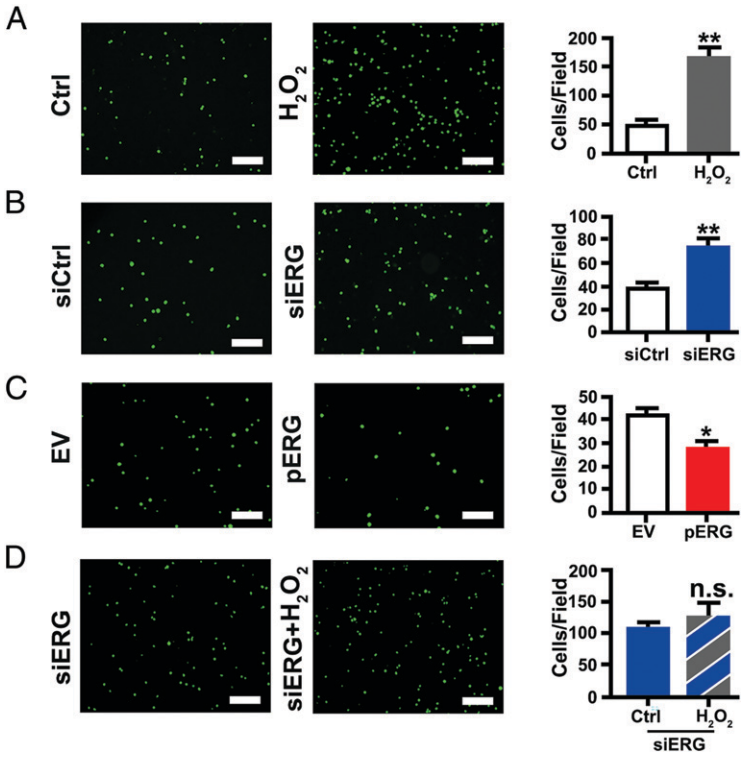

FIGURE 7. ERG negatively regulates THP-1 cell adhesion to HUVECs. HUVECs were cocultured with calcein-AM–labeled THP-1 monocytes for 30 min after exposure to 200 μM H_2O_2 for 12 h (**A**), or transfection with ERG siRNA for 24 h (**B**), or transfection with pERG plasmid for 24 h (**C**). (**D**) HUVECs were transfected with ERG siRNA for 24 h and then treated with 200 μM H_2O_2 for 12 h. THP-1 cell adhesion was captured (left panel) and analyzed (right panel). The number of adherent THP-1 cells is shown as mean ± SEM. Scale bar, 200 μm. $^{*}p < 0.05$, $^{**}p < 0.01$. EV, empty vector.

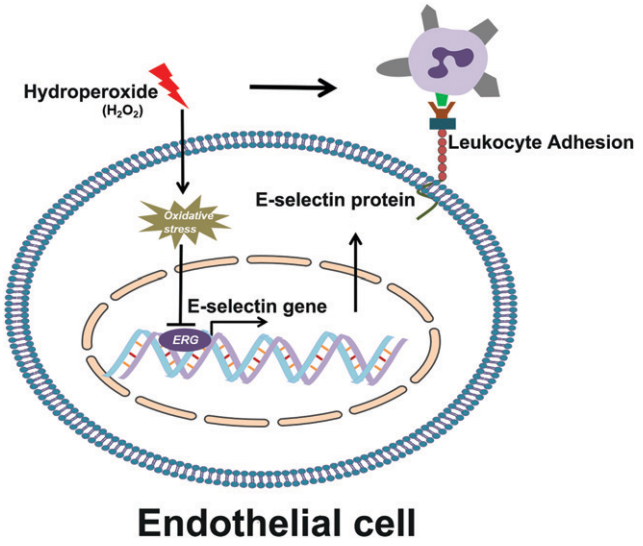

FIGURE 8. Schematic diagram of ERG-regulated E-selectin expression in endothelial cells.

E-selectin promoter and that ERG overexpression resulted in additional binding of ERG to the *E-selectin* promoter. Our results characterized what is, to our knowledge, a novel transcriptional regulator of the *E-selectin* gene (Fig. 8).

ERG is specifically expressed in endothelial cells and abundant in the lung and brain vasculature (56, 57). Inflammatory cytokines TNF-α, LPS, and IL-1β decrease ERG expression in endothelial cells (58–60). Deficiency of ERG increases expression of proinflammatory genes, including *ICAM-1*, *VCAM*, *CD44*, and *IL-8* (33, 60). ERG directly binds to the −75 ETS binding motif on the *IL-8* promoter and inhibits *IL-8* gene transcription (60). Both the −118 and −181 ETS binding motifs on the *ICAM-1* promoter mediate ERG-repressed *ICAM1* gene transcription (33). In addition, overexpression of ERG inhibits the NF-κB signaling pathway, thereby reducing TNF-α–induced ICAM-1 expression at early time points (33). ERG is required for expression of VE-cadherin, von Willebrand factor, endoglin, claudin-5, and thrombomodulin, which contribute to vascular homeostasis (27–29, 31, 32). In our study, we showed that ERG decreases E-selectin expression and mediates oxidative stress–induced monocyte attachment. These results suggest that ERG is a negative regulator for thrombosis.

In summary, our study demonstrates that oxidative stress induces E-selectin expression in endothelial cells via repression of transcription factor ERG and that ERG inhibits the *E-selectin* gene transcription and decreases oxidative stress–induced monocyte adhesion. These findings demonstrate what we believe are novel regulatory mechanisms of E-selectin expression, which may help develop novel therapeutic approaches for thrombotic diseases.

Disclosures

The authors have no financial conflicts of interest.

References

1. Komatsu, T., K. Nagano, S. Sugiura, M. Hagiwara, N. Tanigawa, Y. Abiko, F. Yoshimura, Y. Furuichi, and K. Matsushita. 2012. E-selectin mediates *Porphyromonas gingivalis* adherence to human endothelial cells. *Infect. Immun.* 80: 2570–2576.
2. Gunawan, R. C., D. Almeda, and D. T. Auguste. 2011. Complementary targeting of liposomes to IL-1α and TNF-α activated endothelial cells via the transient expression of VCAM1 and E-selectin. *Biomaterials* 32: 9848–9853.
3. Wiese, G., S. R. Barthel, and C. J. Dimitroff. 2009. Analysis of physiologic E-selectin-mediated leukocyte rolling on microvascular endothelium. *J. Vis. Exp.* (24): 1009.
4. Zanardo, R. C., C. S. Bonder, J. M. Hwang, G. Andonegui, L. Liu, D. Vestweber, L. Zbytnuik, and P. Kubes. 2004. A down-regulatable E-selectin ligand is functionally important for PSGL-1-independent leukocyte-endothelial cell interactions. *Blood* 104: 3766–3773.
5. Sreeramkumar, V., M. Leiva, A. Stadtmann, C. Pitaval, I. Ortega-Rodríguez, M. K. Wild, B. Lee, A. Zarbock, and A. Hidalgo. 2013. Coordinated and unique functions of the E-selectin ligand ESL-1 during inflammatory and hematopoietic recruitment in mice. *Blood* 122: 3993–4001.
6. Hidalgo, A., A. J. Peired, M. Wild, D. Vestweber, and P. S. Frenette. 2007. Complete identification of E-selectin ligands on neutrophils reveals distinct functions of PSGL-1, ESL-1, and CD44. *Immunity* 26: 477–489.
7. Huang, D., Q. Ding, S. Chen, S. Lü, Y. Zhang, and M. Long. 2021. E-selectin negatively regulates polymorphonuclear neutrophil transmigration through altered endothelial junction integrity. *FASEB J.* 35: e21521.
8. Preston, R. C., R. P. Jakob, F. P. Binder, C. P. Sager, B. Ernst, and T. Maier. 2016. E-selectin ligand complexes adopt an extended high-affinity conformation. *J. Mol. Cell Biol.* 8: 62–72.
9. Sullivan, V. V., A. E. Hawley, D. M. Farris, B. S. Knipp, A. J. Varga, S. K. Wrobleski, P. Thanapron, M. J. Eagleton, D. D. Myers, J. B. Fowlkes, and T. W. Wakefield. 2003. Decrease in fibrin content of venous thrombi in selectin-deficient mice. *J. Surg. Res.* 109: 1–7.
10. Culmer, D. L., M. L. Dunbar, A. E. Hawley, S. Sood, R. E. Sigler, P. K. Henke, T. W. Wakefield, J. L. Magnani, and D. D. Myers, Jr. 2017. E-selectin inhibition with GMI-1271 decreases venous thrombosis without profoundly affecting tail vein bleeding in a mouse model. *Thromb. Haemost.* 117: 1171–1181.
11. Galley, H. F., M. G. Blaylock, A. M. Dubbels, and N. R. Webster. 2000. Variability in E-selectin expression, mRNA levels and sE-selectin release between endothelial cell lines and primary endothelial cells. *Cell Biol. Int.* 24: 91–99.
12. Wyble, C. W., K. L. Hynes, J. Kuchibhotla, B. C. Marcus, D. Hallahan, and B. L. Gewertz. 1997. TNF-alpha and IL-1 upregulate membrane-bound and soluble E-selectin through a common pathway. *J. Surg. Res.* 73: 107–112.
13. Yu, G. H., and Y. Fang. 2022. Resveratrol attenuates atherosclerotic endothelial injury through the Pin1/Notch1 pathway. *Toxicol. Appl. Pharmacol.* 446: 116047.
14. Gando, S., S. Nanzaki, Y. Morimoto, S. Kobayashi, and O. Kemmotsu. 2000. Out-of-hospital cardiac arrest increases soluble vascular endothelial adhesion molecules and neutrophil elastase associated with endothelial injury. *Intensive Care Med.* 26: 38–44.
15. Ebert, J., P. Wilgenbus, J. F. Teiber, K. Jurk, K. Schwierczek, M. Döhrmann, N. Xia, H. Li, L. Spiecker, W. Ruf, and S. Horke. 2018. Paraoxonase-2 regulates coagulation activation through endothelial tissue factor. *Blood* 131: 2161–2172.
16. Ketelhuth, D. F., and G. K. Hansson. 2011. Cellular immunity, low-density lipoprotein and atherosclerosis: break of tolerance in the artery wall. *Thromb. Haemost.* 106: 779–786.
17. Sun, J. J., X. W. Yin, H. H. Liu, W. X. Du, L. Y. Shi, Y. B. Huang, F. Wang, C. F. Liu, Y. J. Cao, and Y. L. Zhang. 2018. Rapamycin inhibits ox-LDL-induced inflammation in human endothelial cells in vitro by inhibiting the mTORC2/PKC/c-Fos pathway. *Acta Pharmacol. Sin.* 39: 336–344.
18. Iannantuoni, F., A. M de Marañon, Z. Abad-Jiménez, F. Canet, P. Díaz-Pozo, S. López-Domènech, C. Morillas, M. Rocha, and V. M. Víctor. 2020. Mitochondrial alterations and enhanced human leukocyte/endothelial cell interactions in type 1 diabetes. *J. Clin. Med.* 9: 2155.
19. De Marañon, A. M., F. Iannantuoni, Z. Abad-Jiménez, F. Canet, P. Díaz-Pozo, S. López-Domènech, A. Jover, C. Morillas, G. Mariño, N. Apostolova, et al. 2020. Relationship between PMN-endothelium interactions, ROS production and Beclin-1 in type 2 diabetes. *Redox Biol.* 34: 101563.
20. Masi, S., M. Uliana, and A. Virdis. 2019. Angiotensin II and vascular damage in hypertension: role of oxidative stress and sympathetic activation. *Vascul. Pharmacol.* 115: 13–17.
21. Piqueras, L., and M. J. Sanz. 2020. Angiotensin II and leukocyte trafficking: new insights for an old vascular mediator. Role of redox-signaling pathways. *Free Radic. Biol. Med.* 157: 38–54.
22. von Brühl, M. L., K. Stark, A. Steinhart, S. Chandraratne, I. Konrad, M. Lorenz, A. Khandoga, A. Tirniceriu, R. Coletti, M. Köllnberger, et al. 2012. Monocytes, neutrophils, and platelets cooperate to initiate and propagate venous thrombosis in mice in vivo. *J. Exp. Med.* 209: 819–835.
23. Purdy, M., A. Obi, D. Myers, and T. Wakefield. 2022. P- and E- selectin in venous thrombosis and non-venous pathologies. *J. Thromb. Haemost.* 20: 1056–1066.
24. Heestermans, M., S. Salloum-Asfar, T. Streef, E. H. Laghmani, D. Salvatori, B. M. Luken, S. S. Zeerleder, H. M. H. Spronk, S. J. Korporaal, D. Kirchhofer, et al. 2019. Mouse venous thrombosis upon silencing of anticoagulants depends on tissue factor and platelets, not FXII or neutrophils. *Blood* 133: 2090–2099.
25. Chase, S. D., J. L. Magnani, and S. I. Simon. 2012. E-selectin ligands as mechanosensitive receptors on neutrophils in health and disease. *Ann. Biomed. Eng.* 40: 849–859.
26. Kalna, V., Y. Yang, C. R. Peghaire, K. Frudd, R. Hannah, A. V. Shah, L. Osuna Almagro, J. J. Boyle, B. Göttgens, J. Ferrer, et al. 2019. The transcription factor ERG regulates super-enhancers associated with an endothelial-specific gene expression program. *Circ. Res.* 124: 1337–1349.
27. Birdsey, G. M., N. H. Dryden, V. Amsellem, F. Gebhardt, K. Sahnan, D. O. Haskard, E. Dejana, J. C. Mason, and A. M. Randi. 2008. Transcription factor Erg regulates angiogenesis and endothelial apoptosis through VE-cadherin. *Blood* 111: 3498–3506.
28. Pimanda, J. E., W. Y. Chan, I. J. Donaldson, M. Bowen, A. R. Green, and B. Göttgens. 2006. Endoglin expression in the endothelium is regulated by Fli-1, Erg, and Elf-1 acting on the promoter and a −8-kb enhancer. *Blood* 107: 4737–4745.
29. Liu, F., Q. Liu, F. Yuan, S. Guo, J. Liu, Z. Sun, P. Gao, Y. Wang, S. Yan, and J. Liu. 2019. Erg mediates downregulation of claudin-5 in the brain endothelium of a murine experimental model of cerebral malaria. *FEBS Lett.* 593: 2585–2595.
30. Han, R., M. Pacifici, M. Iwamoto, and M. Trojanowska. 2015. Endothelial Erg expression is required for embryogenesis and vascular integrity. *Organogenesis* 11: 75–86.

31. Liu, J., L. Yuan, G. Molema, E. Regan, L. Janes, D. Beeler, K. C. Spokes, Y. Okada, T. Minami, P. Oettgen, and W. C. Aird. 2011. Vascular bed-specific regulation of the von Willebrand factor promoter in the heart and skeletal muscle. *Blood* 117: 342–351.
32. Peghaire, C., N. P. Dufton, M. Lang, I. I. Salles-Crawley, J. Ahnström, V. Kalna, C. Raimondi, C. Pericleous, L. Inuabasi, R. Kiseleva, et al. 2019. The transcription factor ERG regulates a low shear stress-induced anti-thrombotic pathway in the microvasculature. *Nat. Commun.* 10: 5014.
33. Dryden, N. H., A. Sperone, S. Martin-Almedina, R. L. Hannah, G. M. Birdsey, S. T. Khan, J. A. Layhadi, J. C. Mason, D. O. Haskard, B. Göttgens, and A. M. Randi. 2012. The transcription factor Erg controls endothelial cell quiescence by repressing activity of nuclear factor (NF)-κB p65. *J. Biol. Chem.* 287: 12331–12342.
34. Meng, M., J. Tan, W. Chen, Q. Du, B. Xie, N. Wang, H. Zhu, and K. Wang. 2019. The fibrosis and immunological features of hypochlorous acid induced mouse model of systemic sclerosis. *Front. Immunol.* 10: 1861.
35. Mifsud, B., F. Tavares-Cadete, A. N. Young, R. Sugar, S. Schoenfelder, L. Ferreira, S. W. Wingett, S. Andrews, W. Grey, P. A. Ewels, et al. 2015. Mapping long-range promoter contacts in human cells with high-resolution capture Hi-C. *Nat. Genet.* 47: 598–606.
36. Cairns, J., P. Freire-Pritchett, S. W. Wingett, C. Várnai, A. Dimond, V. Plagnol, D. Zerbino, S. Schoenfelder, B. M. Javierre, C. Osborne, et al. 2016. CHiCAGO: robust detection of DNA looping interactions in Capture Hi-C data. *Genome Biol.* 17: 127.
37. Wingett, S., P. Ewels, M. Furlan-Magaril, T. Nagano, S. Schoenfelder, P. Fraser, and S. Andrews. 2015. HiCUP: pipeline for mapping and processing Hi-C data. *F1000 Res.* 4: 1310.
38. Higashijima, Y., Y. Matsui, T. Shimamura, R. Nakaki, N. Nagai, S. Tsutsumi, Y. Abe, V. M. Link, M. Osaka, M. Yoshida, et al. 2020. Coordinated demethylation of H3K9 and H3K27 is required for rapid inflammatory responses of endothelial cells. *EMBO J.* 39: e103949.
39. Kanki, Y., T. Kohro, S. Jiang, S. Tsutsumi, I. Mimura, J. Suehiro, Y. Wada, Y. Ohta, S. Ihara, H. Iwanari, et al. 2011. Epigenetically coordinated GATA2 binding is necessary for endothelium-specific endomucin expression. *EMBO J.* 30: 2582–2595.
40. Kanki, Y., R. Nakaki, T. Shimamura, T. Matsunaga, K. Yamamizu, S. Katayama, J. I. Suehiro, T. Osawa, H. Aburatani, T. Kodama, et al. 2017. Dynamically and epigenetically coordinated GATA/ETS/SOX transcription factor expression is indispensable for endothelial cell differentiation. *Nucleic Acids Res.* 45: 4344–4358.
41. Miao, Y., N. E. Ajami, T. S. Huang, F. M. Lin, C. H. Lou, Y. T. Wang, S. Li, J. Kang, H. Munkacsi, M. R. Maurya, et al. 2018. Enhancer-associated long non-coding RNA LEENE regulates endothelial nitric oxide synthase and endothelial function. *Nat. Commun.* 9: 292.
42. Son, S. M., M. K. Whalin, D. G. Harrison, W. R. Taylor, and K. K. Griendling. 2004. Oxidative stress and diabetic vascular complications. *Curr. Diab. Rep.* 4: 247–252.
43. Morigi, M., S. Angioletti, B. Imberti, R. Donadelli, G. Micheletti, M. Figliuzzi, A. Remuzzi, C. Zoja, and G. Remuzzi. 1998. Leukocyte-endothelial interaction is augmented by high glucose concentrations and hyperglycemia in a NF-κB-dependent fashion. *J. Clin. Invest.* 101: 1905–1915.
44. Liao, L., R. M. Starzyk, and D. N. Granger. 1997. Molecular determinants of oxidized low-density lipoprotein-induced leukocyte adhesion and microvascular dysfunction. *Arterioscler. Thromb. Vasc. Biol.* 17: 437–444.
45. Li, Y., K. Wang, Y. Feng, C. Fan, F. Wang, J. Yan, J. Yang, H. Pei, Z. Liang, S. Jiang, et al. 2014. Novel role of silent information regulator 1 in acute endothelial cell oxidative stress injury. *Biochim. Biophys. Acta* 1842: 2246–2256.
46. Wassmann, S., U. Laufs, K. Müller, C. Konkol, K. Ahlbory, A. T. Bäumer, W. Linz, M. Böhm, and G. Nickenig. 2002. Cellular antioxidant effects of atorvastatin in vitro and in vivo. *Arterioscler. Thromb. Vasc. Biol.* 22: 300–305.
47. Laridan, E., K. Martinod, and S. F. De Meyer. 2019. Neutrophil extracellular traps in arterial and venous thrombosis. *Semin. Thromb. Hemost.* 45: 86–93.
48. Myers, D., Jr., D. Farris, A. Hawley, S. Wrobleski, A. Chapman, L. Stoolman, R. Knibbs, R. Strieter, and T. Wakefield. 2002. Selectins influence thrombosis in a mouse model of experimental deep venous thrombosis. *J. Surg. Res.* 108: 212–221.
49. Myers, D., Jr., P. Lester, R. Adili, A. Hawley, L. Durham, V. Dunivant, G. Reynolds, K. Crego, Z. Zimmerman, S. Sood, et al. 2020. A new way to treat proximal deep venous thrombosis using E-selectin inhibition. *J. Vasc. Surg. Venous Lymphat. Disord.* 8: 268–278.
50. Devata, S., D. E. Angelini, S. Blackburn, A. Hawley, D. D. Myers, J. K. Schaefer, M. Hemmer, J. L. Magnani, H. M. Thackray, T. W. Wakefield, and S. L. Sood. 2020. Use of GMI-1271, an E-selectin antagonist, in healthy subjects and in 2 patients with calf vein thrombosis. *Res. Pract. Thromb. Haemost.* 4: 193–204.
51. Whitley, M. Z., D. Thanos, M. A. Read, T. Maniatis, and T. Collins. 1994. A striking similarity in the organization of the E-selectin and beta interferon gene promoters. *Mol. Cell. Biol.* 14: 6464–6475.
52. Boyle, E. M., Jr., T. T. Sato, R. F. Noel, Jr., E. D. Verrier, and T. H. Pohlman. 1999. Transcriptional arrest of the human E-selectin gene. *J. Surg. Res.* 82: 194–200.
53. Collins, T., M. A. Read, A. S. Neish, M. Z. Whitley, D. Thanos, and T. Maniatis. 1995. Transcriptional regulation of endothelial cell adhesion molecules: NF-κB and cytokine-inducible enhancers. *FASEB J.* 9: 899–909.
54. Ray, K. P., S. Farrow, M. Daly, F. Talabot, and N. Searle. 1997. Induction of the E-selectin promoter by interleukin 1 and tumour necrosis factor alpha, and inhibition by glucocorticoids. *Biochem. J.* 328: 707–715.
55. Chen, Y. H., Y. H. Huang, H. L. Wu, M. P. Wu, W. T. Chang, Y. Z. Kuo, K. C. Lu, and L. W. Wu. 2008. Angiostatin K1-3 induces E-selectin via AP1 and Ets1: a mediator for anti-angiogenic action of K1-3. *J. Thromb. Haemost.* 6: 1953–1961.
56. Caporarello, N., J. Lee, T. X. Pham, D. L. Jones, J. Guan, P. A. Link, J. A. Meridew, G. Marden, T. Yamashita, C. A. Osborne, et al. 2022. Dysfunctional ERG signaling drives pulmonary vascular aging and persistent fibrosis. [Published erratum appears in 2022 *Nat. Commun.* 13: 5687.] *Nat. Commun.* 13: 4170.
57. Haber, M. A., A. Iranmahboob, C. Thomas, M. Liu, A. Najjar, and D. Zagzag. 2015. ERG is a novel and reliable marker for endothelial cells in central nervous system tumors. *Clin. Neuropathol.* 34: 117–127.
58. Yao, F., Z. Jin, Z. Zheng, X. Lv, L. Ren, J. Yang, D. Chen, B. Wang, W. Yang, L. Chen, et al. 2022. HDAC11 promotes both NLRP3/caspase-1/GSDMD and caspase-3/GSDME pathways causing pyroptosis via ERG in vascular endothelial cells. *Cell Death Discov.* 8: 112.
59. Schafer, C. M., S. Martin-Almedina, K. Kurylowicz, N. Dufton, L. Osuna-Almagro, M. L. Wu, C. F. Johnson, A. V. Shah, D. O. Haskard, A. Buxton, et al. 2023. Cytokine-mediated degradation of the transcription factor ERG impacts the pulmonary vascular response to systemic inflammatory challenge. *Arterioscler. Thromb. Vasc. Biol.* 43: 1412–1428.
60. Yuan, L., V. Nikolova-Krstevski, Y. Zhan, M. Kondo, M. Bhasin, L. Varghese, K. Yano, C. V. Carman, W. C. Aird, and P. Oettgen. 2009. Antiinflammatory effects of the ETS factor ERG in endothelial cells are mediated through transcriptional repression of the interleukin-8 gene. *Circ. Res.* 104: 1049–1057.